

Enhancing carbon sinks in China using a spatially-optimized forestation strategy

Received: 17 September 2024

Accepted: 2 January 2026

Published online: 12 January 2026

 Check for updates

Yanli Dong¹, Zhen Yu^{1,2,3}✉, Thomas Pugh⁴, Evgenios Agathokleous^{1,3,5}, Fangmin Zhang^{1,3}, Stephen Sitch⁶, Weibin You^{7,8}, Wangya Han^{1,3}, Stefan Olin⁴, Shirong Liu^{2,9}, Guoyi Zhou^{1,3}, Pedro Cabral^{1,10} & Pengsen Sun²

China plans expanding 49.5 million hectares of new forests by 2050 to strengthen carbon sequestration. However, estimates of the carbon benefits from this expansion rarely consider the effect of ‘forest edge’, where tree mortality increases under intensified stress from wind, drought, pests, and fire. Here we show that proximity to forest edges substantially reduces biomass carbon storage, and develop a spatial optimization strategy that prioritizes planting in areas that minimize edge effects. Our projections show that forestation optimized for edge effects results in a 51% increase in carbon gain (986 ± 22 Tg by 2060), with approximately half of the total gain driven by reduced edge effects. These findings demonstrate that ignoring edge effects can significantly overestimate carbon sink potential and highlight spatially optimized forestation as a pathway to maximize climate mitigation and ecological benefits.

China severely suffered from ecological and environmental deterioration caused by the overexploitation of forest resources due to rapid economic development^{1,2}. Hence, large-scale greening projects, such as the Grain for Green Program and the Three-North Shelter Forest Program, were implemented to address the challenges of land degradation, desertification, and water and soil retention³. Intensive forestation and management activities helped to expand China’s forest coverage from 12% in 1979 to about 23% in 2019⁴. Forestation practices were prioritized in environmentally vulnerable areas or areas with critical ecological functions initially (i.e., soil retention). As China made progress on environmental goals and the urgency of climate action increases, forestation activities increasingly focus on carbon sequestration. However, initially forestation aimed at environmental enhancement may result in a landscape of disconnected forest

patches. For example, the Grain for Green Program sharply increased the number of forest patches in northwest China⁵.

From an ecological standpoint, the growing patchwork of forests is a sign of fragmentation. This process fragments large habitats into smaller ones and creates more disturbed, unhealthy forest edges^{6,7}. Different from natural edges (adjacent to a relatively permanent non-forest ecosystem devoid of human activity), disturbed forest edges (both natural and developed) may suffer from increased tree mortality and reduced biomass^{8–11}. Moreover, although species diversity and richness were 50–56% greater at both natural and developed forest edges compared to the interior, the abundance of invasive species was nearly twice as high in developed edges¹¹. This indicates that while edges are diverse, those created by development carry a disproportionately high risk of biological invasion. Hence, strategic

¹State Key Laboratory of Climate System Prediction and Risk Management, Nanjing University of Information Science and Technology, Nanjing, China. ²Key Laboratory of Forest Ecology and Environment, China’s National Forestry and Grassland Administration, Ecology and Nature Conservation Institute, Chinese Academy of Forestry, Beijing, China. ³Key Laboratory of Ecosystem Carbon Source and Sink, China Meteorological Administration (ECSS-CMA), School of Ecology and Applied Meteorology, Nanjing University of Information Science and Technology, Nanjing, China. ⁴Department of Physical Geography and Ecosystem Science, Lund University, Lund, Sweden. ⁵Climate and Atmosphere Research Center, The Cyprus Institute, Nicosia, Cyprus. ⁶Faculty of Environment, Science and Economics, University of Exeter, Exeter, UK. ⁷College of Forestry, Fujian Agriculture and Forestry University, Fuzhou, China. ⁸Fujian Southern Forest Resources and Environmental Engineering Technology Research Center, Fujian Agriculture and Forestry University, Fuzhou, China. ⁹Academy of Forestry and Grassland Carbon Sink, Chinese Academy of Forestry, Beijing, China. ¹⁰NOVA Information Management School (NOVA IMS), Universidade Nova de Lisboa, Lisboa, Portugal. ✉ e-mail: zyu@nuist.edu.cn

planning is required to enhance carbon sequestration by mitigating forest edge degradation. This strategic planning is especially important in China, where a substantial proportion of forest edges are shaped by human development, and effective land-use strategies could simultaneously boost carbon storage and curb the threat of invasive species.

The vast majority of the world's forests are influenced by their edges¹². Defined as the boundary between woodland and another land type¹³, these edges are common; over 70% of global forests are within 1 km of non-forest edges¹². Furthermore, a substantial portion of these edges are human-made, created by development and deforestation¹⁴. A majority (over 50%) of global forests underwent an increase in fragmentation between 2000 and 2020¹⁵, implying growing forest edge areas worldwide. Although the continuous forestation projects were not specifically designed to reduce forest edges in China, the expanding forest areas have eased forest fragmentation between 2000 and 2020¹⁶. However, China still exhibits high forest fragmentation due to extensive, disturbed edges. These anthropogenic edges differ fundamentally from natural forest boundaries¹⁶, indicating significant potential for reducing the negative impacts of edge areas through targeted interventions.

Forestation plays a predominant role in retaining land carbon stocks and is the largest contributor to the recent increases in China's land carbon sink^{17–19}. China committed to a massive forestation effort between 2021 and 2050, aiming to create 49.5 million hectares (Mha) of new forest to strengthen its forest carbon sink in pursuit of its 2060 carbon neutrality goal²⁰. However, important uncertainties persist regarding the prioritization of locations, the selection of appropriate tree species, and the potential carbon sequestration gains achievable through a spatially optimized strategy. Forest fragmentation reduces carbon storage in edge areas^{14,21}, suggesting a significant potential for carbon enhancement through edge-reduction strategies¹⁶.

China's forestation plan is at a pivotal turning point, shifting its focus from broad, target-driven expansion for environmental improvement to targeted carbon enhancement. Therefore, smart forestation is essential for forest resilience and climate adaptation. In this work, we hypothesize that fragmentation reduces biomass carbon stocks in China's edge forests. To address these considerations, here we develop a smart forestation strategy to enhance carbon sequestration, utilizing data from the 9th National Forest Inventory (NFI),

which includes more than 3 million measurement records of individual trees from in situ plots (see “Materials and Methods”). Using this dataset, we first calculate carbon stocks for individual trees using provincial, species-specific allometric equations (i.e., biomass-diameter at breast height [DBH] relationships; Supplementary Table 1) and biomass-to-carbon conversion factors^{22–27}. We aggregate these values to the plot level to analyze the spatial patterns of carbon stock variation along forest edge proximity gradients. Using these plot-level data, we develop a machine-learning model to predict forest biomass carbon stocks, incorporating forest age, climate impacts, and edge effects under different forestation and climate scenarios. We then assess the additional carbon benefits of an optimized forestation strategy by comparing its sequestration potential against other scenarios.

Results and discussion

Edge proximity and biomass carbon stock

Based on the NFI data, we found that natural forests were predominantly located within 2.5 km of edges, compared to 1.2 km for planted forests (Fig. 1a). This distribution suggests that forestation efforts have been concentrated either on the periphery of existing forest stands or in newly created, fragmented forest patches. Interestingly, tree biomass carbon stock increased significantly with distance from the forest edge; it was approximately 40% lower in planted forests than in natural forests (Fig. 1a). This aligns with previous findings of lower biomass carbon stock at edges in tropical forests^{10,21,28} but contrasts with observations from temperate U.S. forests, where the biomass carbon stock was higher at edges^{13,29}. The dominant negative impact of forest edge on biomass carbon is further evidenced by a recent global remote-sensing study revealing consistently lower aboveground biomass in edges compared to interiors³⁰. In addition, using logarithmic fitting, we found that forest stand age increases with distance from the edge to the interior (Fig. 1b, $R^2 = 0.69$), a pattern similar to that of forest biomass carbon. However, the age of the planted forest stands shows little variation with increasing distance from the edges (Fig. 1b, $R^2 < 0.01$, $p > 0.05$), suggesting the increasing carbon density in planted forests is not due to the stand age (linear regression: $R^2 = 0.25$, $p > 0.05$).

To clarify the mechanisms shaping the biomass carbon patterns, we examined the types, frequencies, and intensities of different disturbances across distance gradients (Fig. 2). We found that pests and

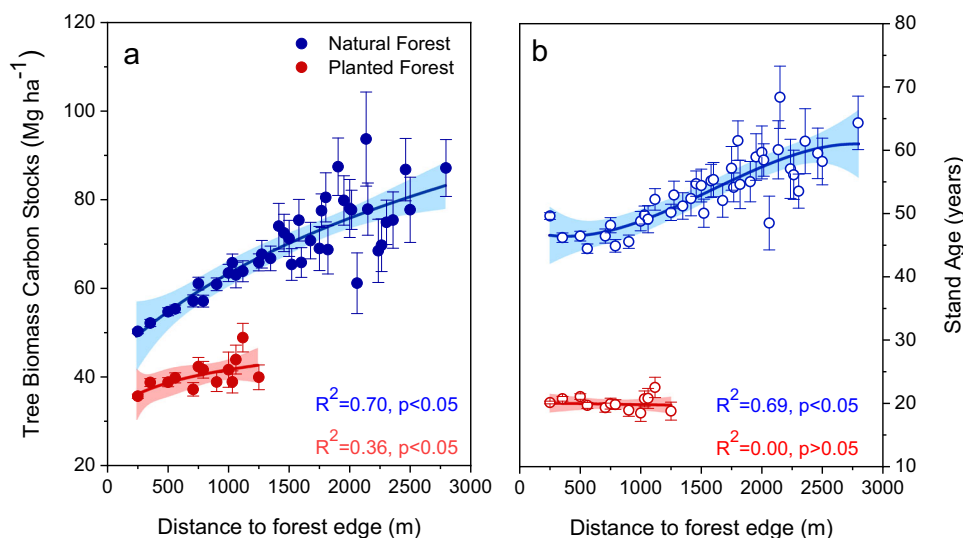


Fig. 1 | Changes in forest biomass carbon stock and stand age along the gradient of the proximity-to-forest edge. **a** Forest biomass carbon; **b** stand age. The error bars represent the mean standard error of samples within the range intervals

automatically generated by R software. The colored shadows represent the 95% confidence intervals of the fitted curves.

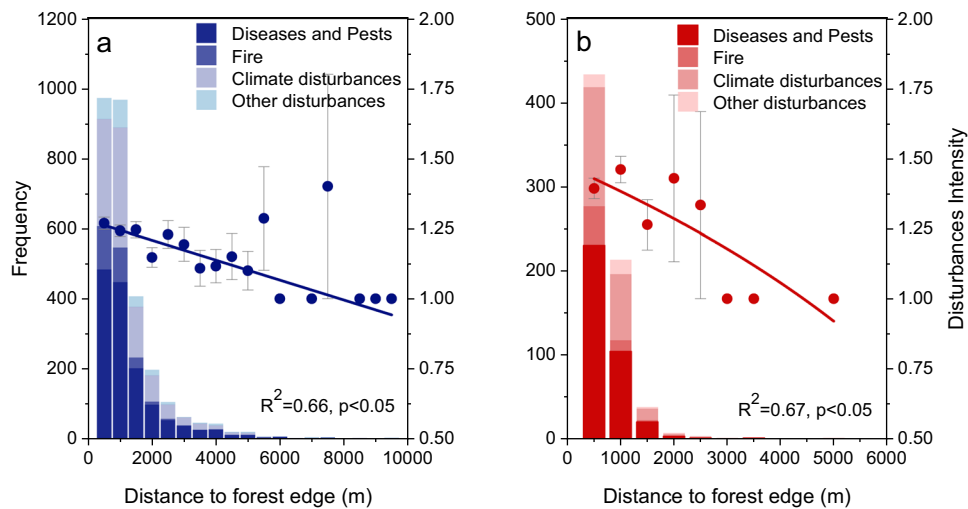


Fig. 2 | Changes in the frequencies, composition, intensities, and types of disturbances along the gradient of proximity to the forest edge. a Natural forests; **b** planted forests. Bar charts and dots represent the frequencies and intensities of

the disturbances. Bar colors represent the types of disturbances. Definitions of disturbance intensities are listed in Supplementary Table 2.

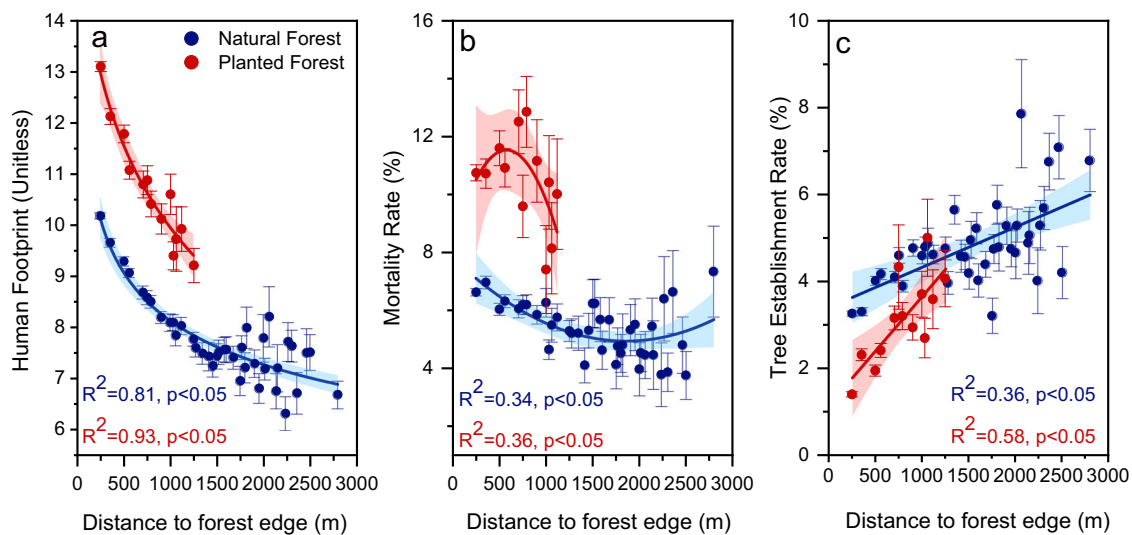


Fig. 3 | Changes in the human footprint, tree mortality rate, and tree establishment rate along the gradient of proximity to the forest edge. a Human footprint; **b** tree mortality rate; **c** tree establishment rate. The tree mortality rate

and establishment rate were calculated as the ratio of dead trees and trees reaching the DBH (biomass-diameter at breast height) threshold of 5 cm between the two inventories.

diseases were the primary stressors in both forest types across distance gradients, followed by climate disturbances and fires (Fig. 2). In addition, the frequency and intensity of disturbances soared with decreasing distance to edges (Fig. 2), indicating much higher disturbance in areas closer to edges. Similarly, we found that the human footprint (the direct and indirect human pressures on the environment due to buildings, population, croplands, roads, railways, etc.) rises sharply from the interior to the edge in both forest types, with a higher human footprint³¹ in planted forests than in natural forests (Fig. 3a). Moreover, tree mortality rates were higher at the edges in both forest types, with planted forests exhibiting a greater rate (7%–13%) than natural forests (4%–7%) within 1 km of the edge (Fig. 3b). In addition, tree establishment rates, as measured by the ratio of trees reaching the DBH threshold of 5 cm between the two inventories, were lower at the edge, which might relate to higher photoinhibition³². Therefore, forest edges are stressed by both human and natural disturbances. These support our hypothesis that China's edge forests have lower biomass carbon stocks due to fragmentation.

Previous studies indicate that edges artificially created by disturbance in young tropical forests negatively affect trees¹⁰, whereas trees in the inherent, longstanding edges of temperate forests often adapt, leveraging increased resource availability for enhanced growth¹³. Therefore, the two contrasting findings observed in the carbon stock patterns between edges and interior areas^{10,13} can be attributed to the varied, disturbance-related, stress levels. The relationship between proximity to forest edges and lower carbon stocks implies a strong link to human disturbances as the primary driver of these low-carbon-density zones.

Forest edges could experience abiotic and biological effects, such as changes in edaphoclimatic conditions and species interactions³³. The negative edge effect on biomass carbon identified in this study can be attributed to the high tree mortality and disturbances between the interior and edges (Figs. 2, 3). For example, forest edges were generally adjacent to lands with low structural complexity (i.e., lower surface roughness), receiving more solar radiation during the daytime but higher re-radiation to the atmosphere at night³⁴, resulting in a higher

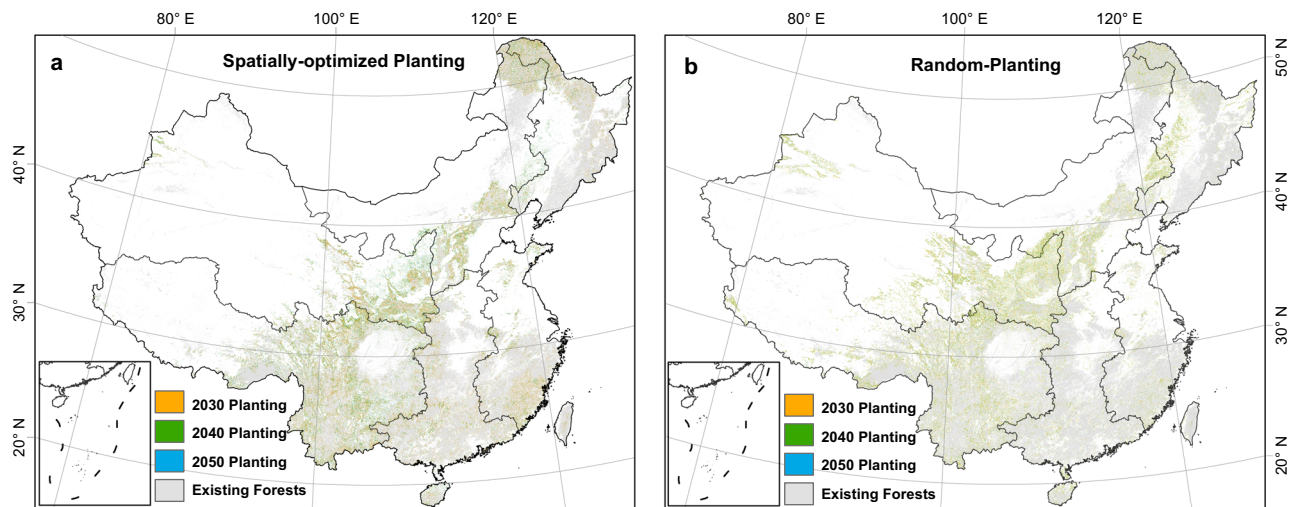


Fig. 4 | Spatial distribution of forestation plans in China. **a** Spatially-optimized scenarios; **b** random-planting scenarios. Yellow, green, and blue pixels represent trees planted by 2030, 2040, and 2050, respectively. The gray pixels represent the existing forests.

wind speed, larger vapor pressure deficit, and greater diurnal fluctuation of soil and air temperature³⁵. Therefore, high mortality rates, especially for tall trees, occur in edge areas^{36–38}. More importantly, the sharp increase in tree mortality rates is related to higher activities of pest insects and diseases at the forest edges, as found in this study (Fig. 2). The high tree mortality might also relate to increasing wind damage and intensified stress of human activity^{39–41}.

Forest edge might also be beneficial for forest stability, especially in natural forest edges. For example, natural forest edges are more stable and therefore might provide more resources to support the growth of vegetation^{42–46}, which could offset potential negative impacts of fragmentation on tree growth⁴⁷. However, such benefits were not confirmed in this study based on a large number of surveyed plots. Consequently, the influence of edge proximity on China's forest biomass carbon stocks more closely resembles the negative relationship observed in tropical forests rather than the positive one documented in U.S. temperate forests^{10,48}. This might be related to the high stress from disturbances at China's forest edges. Thus, our results imply that reducing the forest edge area via a spatially optimized forestation plan would help to enhance the biomass carbon sequestration capacity. This is particularly important in China, which has a long-term strategy of intensive forestation set to continue until 2050²⁰.

Bio-climatically constrained forestation plans

The spatial distribution of potential forest lands must be identified before forest biomass carbon can be accurately estimated. In this study, suitable areas for forestation were identified by applying constraints based on climatic, topological, biological, and edaphic factors, using a random forest (RF) model (Supplementary Fig. 1 and Supplementary Table 3). We found that the potential forestation land was 94.8 Mha in China, with the majority distributed in southwestern (33%), northwestern (29%), and northern areas (15%) (Supplementary Table 4). This differs from the study of Yao et al.⁴⁹, which primarily aimed at carbon stock enhancement through tree densifications in existing forests in southern China. In comparison, our study focuses on establishing new forests through area expansion. Despite differing approaches, our spatially optimized afforestation strategy confirmed southwestern China (39%) as a priority region, consistent with the Hengduan Mountains region (southwestern China) highlighted by Yao et al.⁴⁹.

Our results also showed large contiguous areas of potential forestation lands in the central and northeast regions (Supplementary Fig. 1), which is consistent with previous studies^{3,27,29}. Additionally, our

analysis incorporated indigenous species selection under changing climates. To do so, we examined the distribution suitability of 24 species and species groups (e.g., large monoculture species such as *Pinus massoniana* and mixed forests such as broadleaf mixed forests) under future climate scenarios⁵⁰, which has been widely used in China's forestation projects. For each forestable grid cell, we identified the three most climatically suitable tree species, thereby generating three different forestation schemes for biomass carbon stock estimation (Supplementary Fig. 4).

The optimized scenario demonstrated an advantage over the random-planting scenario through reduced fragmentation and edge effects. Here, priority was placed on planting trees in fragmented, low-edge proximity locations to offset their proximity-to-forest edges under optimized scenario (Fig. 4). An earlier study revealed that a large-scale revegetation program in the region greatly reduced water availability, and tree population could suffer water shortages if vegetation expansion is further intensified⁵¹. Therefore, our optimized forestation strategy was also less intensified in forestation in arid and semi-arid regions (Fig. 4a, b and Supplementary Table 4). Such optimization is achieved using an algorithm to minimize the introduction of new edge areas in contrast to the random forestation strategy (see examples in Supplementary Fig. 3). More specifically, even though the regions have large areas of available land that are bio-climatically suitable for forestation, the optimized forestation strategy would constrain forest expansion in the region and introduce fewer edge areas compared to the non-optimized scenario (Fig. 4).

This study emphasized bioclimatic and ecological constraints in its optimization. For the scenario to be practically implementable, subsequent analyses must integrate economic and accessibility considerations. Thus, the proposed provincial forestation areas differed from those according to the plan released in the National Forest Management Plan (2016–2050)²⁰. However, as implied in this study, we advocate that future national forestation plan could be maneuvered to reduce forest fragmentation for additional benefits.

Project forest biomass carbon stock increment by 2060

The selection of forest species is crucial to accurately predict biomass carbon stock^{3,27,29,50}. We classified the forests into 24 typical tree species and species groups widely adopted in China's forestation projects. Each of the species and species groups was examined to identify the potential distributions under future climate scenarios, using NFI plot observations coupled with machine-learning models²⁷. The top three tree species with the highest suitability for forestation in each

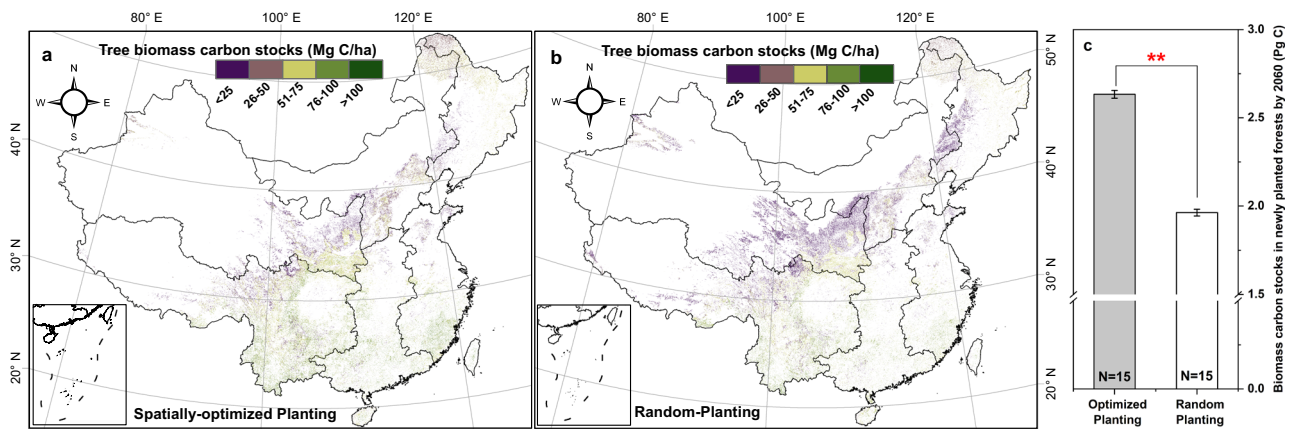


Fig. 5 | Projected tree biomass carbon stock in newly planted forests by 2060. **a** The spatial distributions of biomass carbon density under the spatially-optimized planting scenarios; **b** the spatial distributions of biomass carbon density under random-planting scenarios; **c** the difference in tree biomass carbon stocks between spatially-optimized planting and random-planting scenarios. The error bars

represent the mean standard error of the five climate scenarios (i.e., no climate change, Shared Socioeconomic Pathways (SSP)1-2.6, SSP2-4.5, SSP3-7.0, and SSP5-8.5) for the top three optimal tree species. **** indicates $p < 0.01$. Unit in panel c: Pg (1 Pg = 10^3 Tg).

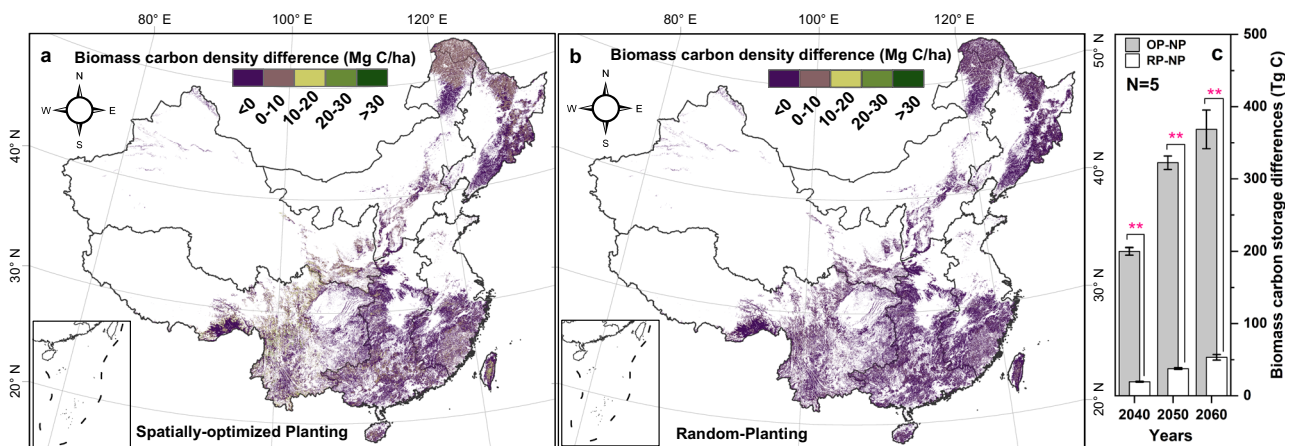


Fig. 6 | Differences in forest biomass carbon density between forestation and non-forestation scenarios. **a** The spatial difference between spatially-optimized planting and non-forestation scenarios; **b** the spatial difference between random-planting and non-forestation scenarios; **c** the difference in national biomass carbon stocks by 2040, 2050, and 2060 under various scenarios (four Shared Socioeconomic Pathways and one scenario with no climate change, $N = 5$). The gray bars

indicate the additional carbon sequestered under a spatially-optimized planting scenario compared to a non-forestation scenario (OP-NP). The white bars indicate the additional carbon sequestered under the random-planting scenario compared to the non-forestation scenario (RP-NP). The error bars represent the mean standard errors of the predictions under different climate change scenarios. **** indicates $p < 0.01$.

forestable grid cell were selected, providing three schemes for forest biomass carbon stock estimates (Supplementary Fig. 4). The RF model was applied to predict the biomass carbon stock of newly planted forests by 2060 by accounting for the impacts of climate, soil, and topographic variables (Fig. 5; see Supplementary Fig. 5 and Supplementary Table 3 for details of the RF model applied). We estimated 986.3 ± 22.2 Tg C (25 Tg C yr^{-1} , or 51.3%) greater forest biomass carbon stock under optimized-planting scenarios, compared to non-optimized scenarios, in which the newly established forest and existing forests contribute 68% and 32%, respectively.

This additional carbon at forest edges will enhance the annual biomass carbon sink by 12.2% from 2021 to 2060^{27,52,53}. Our simulation projects that forest biomass carbon stocks will reach approximately $2,633.3 \pm 20.3$ Tg C by 2060 in newly planted forests created with the optimized-planting strategy (Fig. 5c). This estimate is 34.2% higher than the carbon stock in forests planted with random forestation scenarios ($1,962.3 \pm 18.4$ Tg C, $p < 0.01$, Fig. 5c). Such additional carbon benefits from spatially optimized forestation strategies remain consistent across climate scenarios, despite equivalent forestation areas

between optimized and non-optimized strategies (Fig. 5 and Supplementary Fig. 6). We attribute the carbon stock benefits of newly planted forests to two factors, reduced edge effects and differing spatial distributions (i.e., environmental conditions). Quantitatively, the edge effect accounted for 207.6 ± 6.9 Tg C, while environmental conditions accounted for 463.5 ± 21.2 Tg C (Supplementary Table 5).

In addition to the carbon sink from natural growth in existing forests, spatially optimized forestation activities will also boost carbon sequestration in areas that benefit from reduced edge effects. We found that by 2060, existing forests will retain an additional 53.2 ± 3.9 Tg C under the random-planting approach, compared to non-forestation scenarios. Interestingly, we further found that optimized forestation with the purpose of reducing the edge effect greatly benefits the growth of existing forests, where the additional carbon stock reached a substantially higher level of 368.5 ± 26.7 Tg C (Fig. 6c). Thus, the existing forests will absorb an additional 315.2 ± 23.0 Tg C by 2060 if forestation activities were spatially optimized, compared to random forestation (Fig. 6c). Thus, our results confirm that forest edges are critical for accurately accounting for regional and global carbon

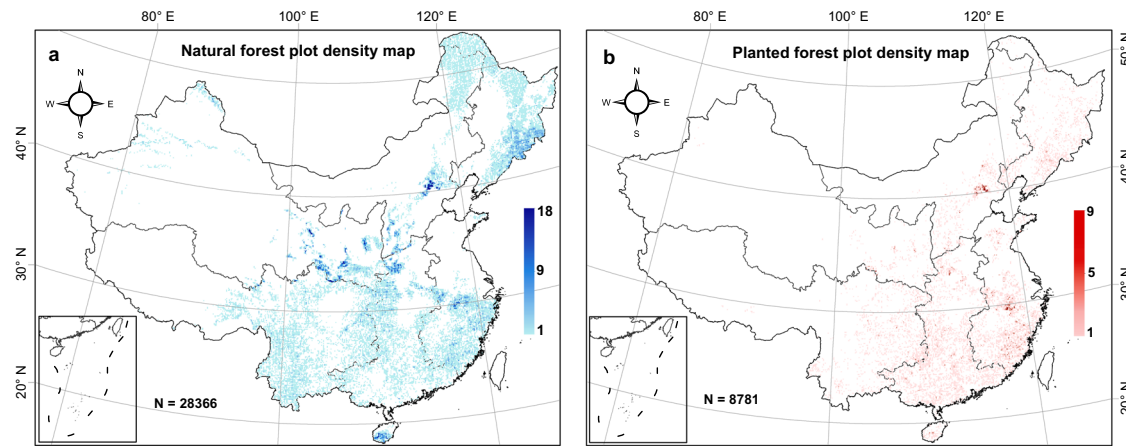


Fig. 7 | Spatial distribution of the forest plots collected and used in this study. a Natural forests; **b** planted forests. The blue and red grids refer to natural forests and planted forests. The depth of the grid color represents the number of forest

plots in each of the 10 km grids. The numbers 28,366 and 8781 are the total plot numbers from natural and planted forests, respectively.

balances, despite their reported and varying impacts^{13,48}. In summary, spatially optimized forestation enhanced carbon stocks by 522.8 ± 28.9 Tg (207.6 Tg from newly planted forests and 315.2 Tg from existing forests) through reduced edge effects, compared to the random-planting scenario, while the remaining 463.5 ± 21.2 Tg increase resulted from allocating forests to locations with more favorable conditions (Supplementary Table 5).

Forests play a central role in achieving the United Nations Sustainable Development Goals, including the sustainable use of terrestrial ecosystems, forest management, combating desertification, reversing land degradation, and halting biodiversity loss^{54,55}. From an ecological perspective, forestation prioritizing planting trees to reduce fragmentation promotes connectivity between forest patches (Supplementary Fig. 7). This would be beneficial for biodiversity conservation according to the percolation theory^{7,56,57}, but it can also accelerate succession, enabling forest edges to develop the characteristics of intact forest more quickly⁵⁸. Our forestation patterns suggest that the spatially optimized forestation significantly reduced the forest patch density (-57.8% , Supplementary Fig. 7) and the perimeter of the forest patch (-15.3% , Supplementary Fig. 7). Such a forestation strategy might also bring auxiliary benefits by mitigating species extinction⁵⁹, carbon emissions⁵⁸, and habitat isolation. Therefore, in addition to the carbon sequestration benefits for existing and newly planted forests, a spatially optimized forestation scheme could also be beneficial for species diversity by reducing pest- and disease-related extinction rates^{44,60} via minimizing forest fragmentation^{44,61}.

In summary, our study revealed that the forest biomass carbon stock declined with an increasing edge effect, depending on the proximity to edges. This pattern was closely related to frequent disturbances, high tree mortality rates, and suppressed tree establishment at forest edges. We further demonstrated that forest biomass carbon stocks can be enhanced through a spatially optimized forestation strategy by reducing forest edge effects and allocating planted forests to locations with more favorable locations. In contrast, neglecting edge effects will lead to carbon stock loss, even though the forested area is virtually the same under different scenarios. It remains uncertain, however, whether edge forests will be more vulnerable to future shifts in disturbance regimes, including fires, and pest outbreaks. In addition, carbon stock predictions are complicated by the combined effects of ongoing forest succession, which continuously reshapes species composition, and climate change-driven shifts in tree competition⁶². Therefore, further studies are needed to better understand disturbances and successional processes to reduce the uncertainty in carbon stock projections. We recommend integrating edge

effects, climate impacts, and spatially smart forest management into conservation and afforestation practices for effective progress toward carbon neutrality.

Methods

Forest plot data

Data from the 9th NFI, 2014–2018), comprising over 3 million measurement records of individual trees across 37,147 plots (Fig. 7), were used, including 28,366 plots from natural forests and 8781 from planted forests. Data on tree species, forest origin, disturbances, DBH, and stand age were essential for this study. Specifically, the disturbance histories were recorded, including the type (e.g., pests, disease, fire) and intensity (scaled from level 1 to 4 with increasing intensity rated based on the proportion of trees affected in a stand; see Supplementary Table 2). We calculated the biomass carbon stock of each tree using DBH and summarized it at the plot level. Tree biomass was estimated for each tree using species-specific allometric equations, which were developed by the State Forestry Administration and tailored to each province (Supplementary Table 1). The proximity of each forest plot to the forest edge was derived from their locations on a land cover map (see below).

Climate data

Where meteorological data (air temperature, precipitation) were missing from forest site measurements, the gaps were filled using gridded datasets acquired from the National Earth System Science Data Center (<https://www.geodata.cn/>) (Supplementary Table 3). The aridity for each site was identified from the Global Aridity Index map at a spatial resolution of 30 arc-seconds (~ 1 km at the equator) (<https://csidotinfo.wordpress.com/>; Global Aridity Index and Potential Evapotranspiration Database V3) (Supplementary Table 3). Moreover, Shared Socioeconomic Pathways (SSP1-2.6, SSP2-4.5, SSP3-7.0, and SSP5-8.5) provided by the Coupled Model Intercomparison Project Phase 6 (CMIP6) were adopted and resampled with a matched spatial resolution (i.e., 250 m) to project forest biomass carbon⁶³.

Topographic data

Missing elevation data in the surveyed forest sites were gap-filled using a 250 m resolution digital elevation model (DEM) from Friedl and Sulla-Menashe⁶⁴ (Supplementary Table 3). The DEM map was also applied to derive related topographical variables, including aspect, slope, and topographic relief. The aforementioned variables served as inputs for the machine-learning model training and the projections of forest biomass carbon (see the next sections).

Soil data and processing

We obtained soil organic carbon, total nitrogen, soil organic matter, and cation exchange capacity from the newly developed 90 m resolution database of the National Soil Information Grids of China (Supplementary Table 3). These variables were used as indicators of soil structure stability, nutrient availability, and the soil capacity to retain nutrients^{65,66}.

Proximity to the forest edge

Two proximity-to-forest edge maps were constructed for this analysis. One map depicted distances from existing forest sites to the nearest edge to examine gradients in biomass carbon stocks. The other represented distances from potential forestation grids to the nearest edge, which was an essential variable for modeling biomass carbon stock projections. Using China Land Use and Cover Change (CNLUCC) data (250 m resolution; see details below), we created maps of proximity to the forest edge, defined as the Euclidean distance from each site/grid to the nearest edge. Analysis of edge effects using CNLUCC maps (2000, 2015, 2018) produced consistent results (Fig. 1 and Supplementary Fig. 8), indicating the robustness of our methodology. Euclidean distance is a commonly adopted definition described with Eq. (1)^{67–69}:

$$d_{(p,q)} = \sqrt{(p_1 - q_1)^2 + (p_2 - q_2)^2} \quad (1)$$

where $d_{(p,q)}$ is the linear distance between the center of a pixel and the center of the nearest source pixel; (p_1, q_1) is the coordinates of the source pixel, and (p_2, q_2) is the coordinates of the nearest source with an attribute value. Proximity-to-forest edge analyses were conducted in ArcGIS (ESRI, USA). The frequency of the number of plots along the proximity-to-edge gradients is shown in Supplementary Fig. 9. Note that forest edges may vary over time due to historically intensive afforestation activities. However, the model framework cannot readily accommodate the dynamic, year-to-year variation in proximity-to-edge metrics are difficult to represent within. Therefore, we used proximity-to-edge data derived from the 2018 CNLUCC map to display the biomass carbon pattern and for model training.

Statistical analysis

The differences in variables between groups were evaluated by independent-sample *t*-test at a significance level of $\alpha = 0.01$. All statistical results are presented as the arithmetic mean \pm standard error of the mean. Data analyses were performed using SPSS 27.0 (IBM Corp., Chicago, IL, USA) and R language; the graphs were drawn in Origin 2018 (Origin Lab, Northampton, MA, USA) and ArcMap 10.2.

Constraints on potential land for forestation

We delineated potential forestation lands by applying various filtering and limiting constraints to existing non-forest areas. First, we identified non-forest areas using the CNLUCC land cover dataset produced by the Institute of Geographic Sciences and Resources of the Chinese Academy of Science²⁹. The CNLUCC dataset was developed using a combination of high-resolution spectral information at 15–30 m from Landsat TM (Thematic Mapper) and Huanjing-1 satellite images⁷⁰. Second, based on the 30-m CNLUCC land cover data, we restricted forestable lands to gridcells of grassland, unused land, and tidal flats, while excluding those identified as cropland, urban, water bodies, and alpine steppe meadows. Third, areas were excluded based on climatic and topographic constraints derived from previous studies; specifically, those with an average annual precipitation of <350 mm or an elevation > 4.9 km^{29,71,72}.

Based on the potential forestable map, we further calculated the suitability index for each gridcell using a machine-learning model by taking into account the climatic, topological, biological, and edaphic

factors. Specifically, we flagged forestation failure plots and normal plots in model training, representing low and high forestation suitability, respectively. We classified lands as forestation failure sites if tree survival rates fell below 41%, a threshold that necessitates reforestation efforts. The trained RF model was then applied to the potential forestable map delineated in the previous step, producing a suitability map for locating the planted area (Supplementary Figs. 1 and 2).

Biomass carbon predictions

This study focuses on the impact of forestation on biomass carbon stock. Therefore, the biomass carbon stocks in the areas affected by forestation were examined, including the newly forested lands and the existing forests in close proximity to the newly forested areas. An RF model was constructed to predict the biomass carbon stocks using in situ measurements for model training^{73–75}. Machine-learning models, such as RF, SVR, artificial neural networks, and gradient boosted regression trees, are used to predict the spatial characteristics of forest cover patterns. Among these models, the RF model consistently outperforms others when modeling complex environmental data^{67,76}. To construct the regression tree, the RF model utilizes bootstrap samples and selects a subset from the original dataset to split the tree nodes, which ultimately refines the regression tree⁷⁵. Note that a few parameters need to be settled, including *mtry*, which denotes the number of features considered by each decision tree during node splitting, and *ntree*, which indicates the number of trees generated, usually set at 500 individuals. The model ranks the importance of variables by % IncMSE and IncNodePurity⁷³ (Supplementary Fig. 5).

In our simulations, we screened the environmental variables used for training and identified 15 predictor variables for inclusion in the prediction model, covering five categories: vegetation, terrain, climate, soil, and other data (Supplementary Table 3). During the model simulation, 70% of the plots were used for model training, while the remaining 30% were used for model validation. The accuracy of the predicted model was $R^2 = 0.78$ and $\text{RMSD} = 29.08 \text{ Mg C ha}^{-1}$ (Supplementary Fig. 5d). Furthermore, we found that stand age and tree density contributed significantly to the predictive model (Supplementary Fig. 5a and c). In addition, a bootstrap sample set was randomly drawn with replacement from the original training data, and the number of trees (*ntree*) was set to 500 (Supplementary Fig. 5b).

Design of simulation experiments

We conducted three groups of experiments to simulate carbon stock changes under various forestation scenarios in China (2021–2060), using a pre-trained machine-learning model. The first group of experiments was based on the assumption that no forestation activities would be implemented under five climate scenarios (i.e., no climate change scenarios and four Shared Socioeconomic Pathways, namely SSP1-2.6, SSP2-4.5, SSP3-7.0, and SSP5-8.5). The second represented a baseline of unplanned (random) forestation, while the third applied a spatially smart forestation strategy to the same total land area, with the objective of reducing proximity to forest edges. Both the second and the third groups were designed to achieve the forestation goal of expanding the forest area by 49.5 Mha from 2021 to 2050 as mandated by the State Forestry Administration²⁰. All experimental groups employed machine-learning models to predict the biomass carbon of existing forests in 2040, 2050, and 2060 (Fig. 6), and assess edge effects on current forest growth. For each simulation, the proximity shall be recalculated after forestation to ensure that the continuous forestation activities follow the rules of reducing edge effects (Supplementary Fig. 2). We quantified the contributions of random and smart forestation strategies to carbon stock by comparing the simulation results from the first and second groups, and then the second and third groups.

Furthermore, for the second and third experimental groups, we conducted simulations with and without edge effects. According to the government guidelines²⁰, both forestation scenarios are implemented to achieve a phased expansion: 28.4 Mha within 250 m of the forest edge by 2030, followed by an additional 13.9 Mha within 500 m by 2040 and 7.6 Mha within about 700 m by 2050 (Supplementary Fig. 2). For each group simulation, we included three species-selection-based forestation schemes (Supplementary Fig. 4), which were used to estimate the biomass carbon stock of newly established forests by 2060 (Fig. 5). All the simulations were performed considering the changes in forest age, species, and climate change impacts at a resolution of 250 × 250 m. For SSPs in second and third experimental groups, we conducted three replicate experiments per pathway using the top three climatically suitable species.

Data availability

The historical climate data is available from <https://data.tpdc.ac.cn/>. The future climate data is provided at: <https://cds.climate.copernicus.eu/>. The land cover maps used are the China Land Use and Cover Change dataset, which can be obtained from the Data Center for Resources and Environmental Sciences, Chinese Academy of Sciences: <http://www.resdc.cn>. The soil data is available from <https://soil.geodata.cn/>. The administrative boundary data were obtained from <https://cloudcenter.tianditu.gov.cn>. The national forest inventory data are protected and are not publicly available due to data privacy laws.

References

- Bryan, B. A. et al. China's response to a national land-system sustainability emergency. *Nature* **559**, 193–204 (2018).
- Delang, C. O. & Yuan, Z. *China's Grain for Green Program: A Review of the Largest Ecological Restoration and Rural Development Program in the World*. (Springer International Publishing, 2015).
- Zhang, L., Sun, P., Huettmann, F. & Liu, S. Where should China practice forestry in a warming world?. *Glob. Change Biol.* **28**, 2461–2475 (2022).
- State Forestry Administration of the People's Republic of China. *Ninth National Forest Resource Inventory Report (2014–2018)* (China Forestry Publishing House, 2019).
- Yang, Z. et al. Spatiotemporal pattern of forest fragmentation in the Loess Plateau. *Resoures Sci.* **40**, 1246–1255 (2018).
- Guo, J. et al. Changes of Chinese forest-grassland ecotone in geographical scope and landscape structure from 1990 to 2020. *Ecography* **2024**, e07296 (2024).
- Taubert, F. et al. Global patterns of tropical forest fragmentation. *Nature* **554**, 519–522 (2018).
- Laurance, W. F. et al. Biomass collapse in Amazonian forest fragments. *Science* **278**, 1117–1118 (1997).
- Jönsson, M. T. et al. Eighteen years of tree mortality and structural change in an experimentally fragmented Norway spruce forest. *For. Ecol. Manag.* **242**, 306–313 (2007).
- Ordway, E. M. & Asner, G. P. Carbon declines along tropical forest edges correspond to heterogeneous effects on canopy structure and function. *PNAS* **117**, 7863–7870 (2020).
- Franklin, C. M. A., Harper, K. A. & Clarke, M. J. Trends in studies of edge influence on vegetation at human-created and natural forest edges across time and space. *Can. J. For. Res.* **51**, 274–282 (2021).
- Haddad, N. M. et al. Habitat fragmentation and its lasting impact on Earth's ecosystems. *Sci. Adv.* **1**, e1500052 (2015).
- Morreale, L. L., Thompson, J. R., Tang, X., Reinmann, A. B. & Hutyrá, L. R. Elevated growth and biomass along temperate forest edges. *Nat. Commun.* **12**, 7181 (2021).
- Brinck, K. et al. High resolution analysis of tropical forest fragmentation and its impact on the global carbon cycle. *Nat. Commun.* **8**, 14855 (2017).
- Zou, Y. et al. Fragmentation increased in over half of global forests from 2000 to 2020. *Science* **389**, 1151–1156 (2025).
- Ma, J., Li, J., Wu, W. & Liu, J. Global forest fragmentation change from 2000 to 2020. *Nat. Commun.* **14**, 3752 (2023).
- Wang, Y. et al. The size of the land carbon sink in China. *Nature* **603**, E7–E9 (2022).
- Fang, J., Yu, G., Liu, L., Hu, S. & Chapin, F. S. 3rd. Climate change, human impacts, and carbon sequestration in China. *PNAS* **115**, 4015–4020 (2018).
- Yu, Z. et al. Forest expansion dominates China's land carbon sink since 1980. *Nat. Commun.* **13**, 5374 (2022).
- State Forestry Administration of the People's Republic of China. *National Forest Management Plan (2016–2050)* (China Forestry Publishing House, 2016).
- Chaplin-Kramer, R. et al. Degradation in carbon stocks near tropical forest edges. *Nat. Commun.* **6**, 10158 (2015).
- Lu, J. *Estimation of Carbon Storage of Arbor Forest Based on the Forest Resource Inventory Data* (Beijing Forestry University, 2020).
- Piao, S. et al. The carbon balance of terrestrial ecosystems in China. *Nature* **458**, 1009–1013 (2009).
- Fang, J., Liu, G. & Xu, S. Biomass and net production of forest vegetation in China. *Acta Ecol. Sin.* **16**, 497–508 (1996).
- Li, H. & Lei, Y. *Estimation and Evaluation of Forest Biomass Carbon Storage in China* (China Forestry Publishing House, 2010).
- Yang, Q. Estimating forest carbon storage in Xiuyan County by forest stock volume biomass model (In Chinese). *Green. Technol.* **23**, 20–22 (2021).
- Yu, Z. et al. Maximizing carbon sequestration potential in Chinese forests through optimal management. *Nat. Commun.* **15**, 3154 (2024).
- Saeed, S. et al. Forest edge effect on biomass carbon along altitudinal gradients in Chinese Fir (*Cunninghamia lanceolata*): a study from Southeastern China. *Carbon Manag.* **10**, 11–22 (2019).
- Xu, H., Yue, C., Zhang, Y., Liu, D. & Piao, S. Forestation at the right time with the right species can generate persistent carbon benefits in China. *PNAS* **120**, e2304988120 (2023).
- Yang, G., Crowther, T., Lauber, T., Zohner, C. & Smith, G. A globally consistent negative effect of edge on aboveground forest biomass. *Nat. Ecol. Evol.* <https://doi.org/10.1038/s41559-025-02840-2> (2025).
- Venter, O. et al. Global terrestrial Human Footprint maps for 1993 and 2009. *Sci. Data* **3**, 160067 (2016).
- Kitao, M. et al. Springtime photoinhibition constrains regeneration of forest floor seedlings of *Abies sachalinensis* after a removal of canopy trees during winter. *Sci. Rep.* **8**, 6310 (2018).
- Murcia, C. Edge effects in fragmented forests: implications for conservation. *Trends Ecol. Evol.* **10**, 58–62 (1995).
- Geiger, R., Aron, R. H. & Todhunter, P. *The Climate Near the Ground, Sixth Edition* (Rowman & Littlefield, 2009).
- Davies-Colley, R. J., Payne, G. W. & van Elswijk, M. Microclimate gradients across a forest edge. *N. Z. J. Ecol.* **24**, 111–121 (2000).
- Esseen, P.-A. Tree mortality patterns after experimental fragmentation of an old-growth conifer forest. *Biol. Conserv.* **68**, 19–28 (1994).
- D'Angelo, S. A., Andrade, A. C. S., Laurance, S. G., Laurance, W. F. & Mesquita, R. C. G. Inferred causes of tree mortality in fragmented and intact Amazonian forests. *J. Trop. Ecol.* **20**, 243–246 (2004).
- Sampaio, A. B. & Scariot, A. O. Edge effect on tree diversity, composition and structure in a deciduous dry forest in Central Brazil. *Rev. Arvore.* **35**, 1121–1134 (2011).
- Fowler, H. G., Silva, C. A. & Venticinque, E. Size, taxonomic and biomass distributions of flying insects in Central Amazonia: forest edge vs. understorey. *Rev. Biol. Trop.* **41**, 755–760 (1993).

40. Brown, K. S., Jr. & Hutchings, R. Disturbance, fragmentation, and the dynamics of diversity in Amazonian forest butterflies. In *Tropical Forest Remnants - Ecology, Management, and Conservation of Fragmented Communities* (eds. Laurance, W. F. & Bierregaard, R. O., Jr.) (University of Chicago Press, 1997).
41. Laurance, W. F., Ferreira, L. V., Rankin-de Merona, J. M. & Laurance, S. G. Rain forest fragmentation and the dynamics of Amazonian tree communities. *Ecology* **79**, 2032–2040 (1998).
42. Kapos, V., Wandelli, E., Camargo, J. L. C. & Ganade, G. M. S. Edge-related changes in environment and plant responses due to forest fragmentation in central Amazonia. In *Tropical Forest Remnants - Ecology, Management, and Conservation of Fragmented Communities* (eds. Laurance, W. F. & Bierregaard, R. O., Jr.) (University of Chicago Press, 1997).
43. Camargo, J. L. C. & Kapos, V. Complex edge effects on soil moisture and microclimate in Central Amazonian forest. *J. Trop. Ecol.* **11**, 205–221 (1995).
44. Laurance, W. F. et al. Ecosystem decay of Amazonian forest fragments: a 22-year investigation. *Conserv. Biol.* **16**, 605–618 (2002).
45. de Paula, M. D., Costa, C. P. A. & Tabarelli, M. Carbon storage in a fragmented landscape of Atlantic forest: the role played by edge-affected habitats and emergent trees. *Trop. Conserv. Sci.* **4**, 349–358 (2011).
46. Pütz, S., Groeneveld, J., Alves, L. F., Metzger, J. P. & Huth, A. Fragmentation drives tropical forest fragments to early successional states: a modelling study for Brazilian Atlantic forests. *Ecol. Model.* **222**, 1986–1997 (2011).
47. Li, W. et al. Human fingerprint on structural density of forests globally. *Nat. Sustain.* **6**, 368–379 (2023).
48. Reinmann, A. B. & Hutrya, L. R. Edge effects enhance carbon uptake and its vulnerability to climate change in temperate broadleaf forests. *PNAS* **114**, 107–112 (2017).
49. Yao, L. et al. Carbon sequestration potential of tree planting in China. *Nat. Commun.* **15**, 8398 (2024).
50. Zhang, L. et al. The use of classification and regression algorithms using the random forests method with presence-only data to model species' distribution. *MethodsX* **6**, 2281–2292 (2019).
51. Feng, X. et al. Revegetation in China's Loess Plateau is approaching sustainable water resource limits. *Nat. Clim. Change* **6**, 1019–1022 (2016).
52. Huang, Y. et al. The role of China's terrestrial carbon sequestration 2010–2060 in offsetting energy-related CO₂ emissions. *Natl. Sci. Rev.* **9**, nwac057 (2022).
53. Cai, W. et al. Carbon sequestration of Chinese forests from 2010 to 2060 spatiotemporal dynamics and its regulatory strategies. *Sci. Bull.* **67**, 836–843 (2022).
54. Department of Economic and Social Affairs. *Forests* (United Nations, last accessed: 5 June 2023); <https://sdgs.un.org/topics/forests>.
55. The International Union for Conservation of Nature (IUCN). *Nature 2030: A Programme for the Union 2021–2024* (IUCN, 2021).
56. Dietrich, S. & Amnon, A. *Introduction to Percolation Theory (2nd Edition)* (Taylor & Francis, 1994).
57. Christensen, K. & Moloney, N. R. *Complexity and Criticality* (Imperial College Press, 2005).
58. Fischer, R. et al. Accelerated forest fragmentation leads to critical increase in tropical forest edge area. *Sci. Adv.* **7**, eabg7012 (2021).
59. Wearn, O. R., Reuman, D. C. & Ewers, R. M. Extinction debt and windows of conservation opportunity in the Brazilian Amazon. *Science* **337**, 228–232 (2012).
60. MacArthur, R. O. & Wilson, E. O. *The Theory of Island Biogeography* (Princeton University Press, 1967).
61. Debinski, D. M. & Holt, R. D. A survey and overview of habitat fragmentation experiments. *Conserv. Biol.* **14**, 342–355 (2000).
62. Dong, Y., Yu, Z., Agathokleous, E., Zhou, G. & Liu, S. Pitfalls in forest carbon sink projection. *J. For. Res.* **35**, 87 (2024).
63. The World Climate Research Plan Working Group. *CMIP6 - Coupled Model Intercomparison Project Phase 6*. <https://pcmdi.llnl.gov/CMIP6/> (2020).
64. Friedl, M. & Sulla-Menashe, D. *Data from MCD12Q1 MODIS Terra/Aqua Land Cover Type Yearly L3 Global 500 m SIN Grid V006* (The Land Processes Distributed Active Archive Center (LP DAAC), NASA, 2021).
65. Khaledian, Y. et al. Modeling soil cation exchange capacity in multiple countries. *CATENA* **158**, 194–200 (2017).
66. Yu, Z. et al. China's forestation on marginal land was less efficient in carbon sequestration compared with non-marginal land. *One Earth* **6**, 1692–1702 (2023).
67. Cohen, D. *Precalculus: A Problems-Oriented Approach* (Cengage Learning, 2004).
68. Liberti, L. & Lavor, C. *Euclidean Distance Geometry: An Introduction* (Springer, 2017).
69. Richmond, T. *General Topology: An Introduction* (De Gruyter, 2020).
70. Liu, J. et al. Spatial patterns and driving forces of land use change in China during the early 21st century. *J. Geog. Sci.* **20**, 483–494 (2010).
71. Liang, E. et al. Species interactions slow warming-induced upward shifts of treelines on the Tibetan Plateau. *PNAS* **113**, 4380–4385 (2016).
72. Li, X. et al. Warming-induced phenological mismatch between trees and shrubs explains high-elevation forest expansion. *Natl. Sci. Rev.* **10**, nwad182 (2023).
73. Wang, X. et al. Quantifying multi-decadal change of planted forest cover using airborne LiDAR and Landsat imagery. *Remote Sens.* **8**, 62 (2016).
74. Simard, M., Pinto, N., Fisher, J. & Baccini, A. Mapping forest canopy height globally with spaceborne LiDAR. *J. Geophys. Res. Biogeosci.* **116**, 4021 (2011).
75. Fassnacht, F. E. et al. Importance of sample size, data type and prediction method for remote sensing-based estimations of aboveground forest biomass. *Remote Sens. Environ.* **154**, 102–114 (2014).
76. Liu, B., Gao, L., Li, B., Marcos-Martinez, R. & Bryan, B. A. Nonparametric machine learning for mapping forest cover and exploring influential factors. *Landsc. Ecol.* **35**, 1683–1699 (2020).

Acknowledgements

This study was supported by National Key Research and Development Program of China (No. 2021YFD2200405 (S.R.L.)), China National Science Foundation (No. 32361143869 (Z.Y.), 32371663 (Z.Y.)), and Jiangsu Provincial Fund for Distinguished Young Scholars (BK20250044) (Z.Y.).

Author contributions

Z.Y. conceived and designed the research. Y.L.D. performed simulations and drew figures. Z.Y. and Y.L.D. wrote the first draft together. E.A., S.R.L., T.P., S.S., and W.B.Y. extensively edited the manuscript. G.Y.Z., F.M.Z., W.Y.H., S.O., P.C., and P.S.S. provided essential suggestions to improve the manuscript.

Competing interests

The authors declare no competing interests.

Additional information

Supplementary information The online version contains supplementary material available at <https://doi.org/10.1038/s41467-026-68288-5>.

Correspondence and requests for materials should be addressed to Zhen Yu.

Peer review information *Nature Communications* thanks Xiaoming Feng, Onkar Ramesh Salunkhe, and the other, anonymous, reviewer(s) for their contribution to the peer review of this work. A peer review file is available.

Reprints and permissions information is available at <http://www.nature.com/reprints>

Publisher's note Springer Nature remains neutral with regard to jurisdictional claims in published maps and institutional affiliations.

Open Access This article is licensed under a Creative Commons Attribution-NonCommercial-NoDerivatives 4.0 International License, which permits any non-commercial use, sharing, distribution and reproduction in any medium or format, as long as you give appropriate credit to the original author(s) and the source, provide a link to the Creative Commons licence, and indicate if you modified the licensed material. You do not have permission under this licence to share adapted material derived from this article or parts of it. The images or other third party material in this article are included in the article's Creative Commons licence, unless indicated otherwise in a credit line to the material. If material is not included in the article's Creative Commons licence and your intended use is not permitted by statutory regulation or exceeds the permitted use, you will need to obtain permission directly from the copyright holder. To view a copy of this licence, visit <http://creativecommons.org/licenses/by-nc-nd/4.0/>.

© The Author(s) 2026